NASA/TM-2005-213521

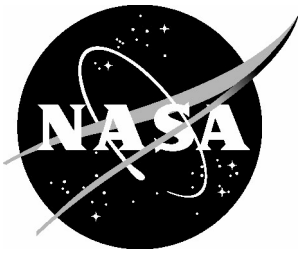

Comparison of Fiber Optic Strain Demodulation Implementations

Cuong C. Quach and Sixto L. Vazquez
Langley Research Center, Hampton, Virginia

March 2005

The NASA STI Program Office . . . in Profile

Since its founding, NASA has been dedicated to the advancement of aeronautics and space science. The NASA Scientific and Technical Information (STI) Program Office plays a key part in helping NASA maintain this important role.

The NASA STI Program Office is operated by Langley Research Center, the lead center for NASA's scientific and technical information. The NASA STI Program Office provides access to the NASA STI Database, the largest collection of aeronautical and space science STI in the world. The Program Office is also NASA's institutional mechanism for disseminating the results of its research and development activities. These results are published by NASA in the NASA STI Report Series, which includes the following report types:

- TECHNICAL PUBLICATION. Reports of completed research or a major significant phase of research that present the results of NASA programs and include extensive data or theoretical analysis. Includes compilations of significant scientific and technical data and information deemed to be of continuing reference value. NASA counterpart of peer-reviewed formal professional papers, but having less stringent limitations on manuscript length and extent of graphic presentations.

- TECHNICAL MEMORANDUM. Scientific and technical findings that are preliminary or of specialized interest, e.g., quick release reports, working papers, and bibliographies that contain minimal annotation. Does not contain extensive analysis.

- CONTRACTOR REPORT. Scientific and technical findings by NASA-sponsored contractors and grantees.

- CONFERENCE PUBLICATION. Collected papers from scientific and technical conferences, symposia, seminars, or other meetings sponsored or co-sponsored by NASA.

- SPECIAL PUBLICATION. Scientific, technical, or historical information from NASA programs, projects, and missions, often concerned with subjects having substantial public interest.

- TECHNICAL TRANSLATION. English-language translations of foreign scientific and technical material pertinent to NASA's mission.

Specialized services that complement the STI Program Office's diverse offerings include creating custom thesauri, building customized databases, organizing and publishing research results ... even providing videos.

For more information about the NASA STI Program Office, see the following:

- Access the NASA STI Program Home Page at ***http://www.sti.nasa.gov***

- E-mail your question via the Internet to help@sti.nasa.gov

- Fax your question to the NASA STI Help Desk at (301) 621-0134

- Phone the NASA STI Help Desk at (301) 621-0390

- Write to:
  NASA STI Help Desk
  NASA Center for AeroSpace Information
  7121 Standard Drive
  Hanover, MD 21076-1320

NASA/TM-2005-213521

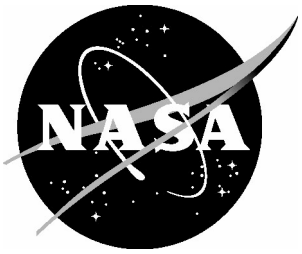

Comparison of Fiber Optic Strain Demodulation Implementations

Cuong C. Quach and Sixto L. Vazquez
Langley Research Center, Hampton, Virginia

National Aeronautics and
Space Administration

Langley Research Center
Hampton, Virginia 23681-2199

March 2005

Available from:

NASA Center for AeroSpace Information (CASI)
7121 Standard Drive
Hanover, MD 21076-1320
(301) 621-0390

National Technical Information Service (NTIS)
5285 Port Royal Road
Springfield, VA 22161-2171
(703) 605-6000

Abstract

NASA Langley Research Center is developing instrumentation based upon principles of Optical Frequency-Domain Reflectometry (OFDR) for the provision of large-scale, dense distribution of strain sensors using fiber optics embedded with Bragg gratings. Fiber Optic Bragg Grating technology enables the distribution of thousands of sensors immune to moisture and electromagnetic interference with negligible weight penalty. At Langley, this technology provides a key component for research and development relevant to comprehensive aerospace vehicle structural health monitoring. A prototype system is under development that includes hardware and software necessary for the acquisition of data from an optical network and conversion of the data into strain measurements.

This report documents the steps taken to verify the software that implements the algorithm for calculating the fiber strain. Brief descriptions of the strain measurement system and the test article are given. The scope of this report is the verification of software implementations as compared to a reference model. The algorithm will be detailed along with comparison results.

Introduction

NASA Langley Research Center (LaRC) is developing instrumentation based upon principles of Optical Frequency-Domain Reflectometry (OFDR) for the provision of large-scale, densely-distributed strain sensors using fiber optics embedded with Bragg gratings. The theory and development of this technology, called the Fiber Optic Strain System (FOSS) is described in [1]. A simple explanation of the fundamental technique is that it identifies the position of a Bragg grating by measuring the free spectral range formed by the grating's reflection and the reflection from a known reference mirror [1]. The resultant signal as a function of wave number has a frequency proportional to the distance between the reference mirror and the grating. A Fourier Transform of the signal will produce a peak at the location of the grating. Fiber Optic Bragg Grating technology enables the distribution of thousands of sensors immune to moisture and electromagnetic interference with negligible weight penalty. At LaRC, this technology provides a key component for research and development relevant to comprehensive aerospace vehicle structural health monitoring. A prototype system currently exists at LaRC that includes hardware and software necessary for the acquisition of data from an optical network and conversion of the data into strain measurements. To be deployed for vehicle structural health monitoring, FOSS must be matured to operate in a real-time environment. Before such a system can be deployed, it is necessary to verify that key software components are computing strain values in accordance with established metrics.

This report documents the steps taken to verify the software that implements the algorithm for calculating the fiber strain based on the work described in [1]. Brief descriptions of the strain measurement system and the test article are given. The scope of this report is the verification of software implementations as compared to a reference model. The algorithm will be detailed along with comparison results.

General System Description

In an effort to record and display near real-time measurements, the prototype system distributes data acquisition, strain computation, data display, archiving and other tasks across multiple computers connected through a shared-memory architecture as illustrated in Figure 1.

The processing cycle begins with high-speed data acquisition hardware reading the grating reflections from a photo detector during the laser's frequency sweep. The acquired data is then posted to the shared memory network enabling immediate access by all network nodes - the node performing the archiving can begin writing out data while simultaneously another node performs the strain processing function.

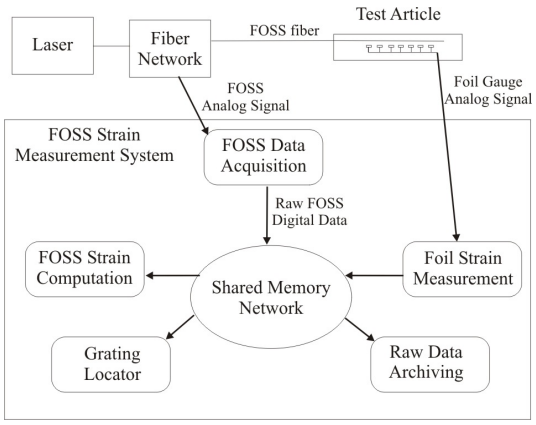

Figure 1: *Topology for Fiber Strain Measurement System.*

One of the reasons for using a distributed architecture is to reduce the cycle time from the data acquisition to strain reporting. By dedicating separate CPUs to specific functions, data dependent functions such as data acquisition and processing, can be pipelined; and non-data dependent tasks, such as display and archiving, can be simultaneously executed.

This necessitates strong coordination amongst the separate components so that data can flow smoothly between nodes. The nodes are connected through a reflective memory network (SCRAMNet). The data transfer rate is an important selection parameter because of the voluminous data involved with each scan of a single fiber. The size of each scan is 1,048,576 floating-point values, equating to 4 MB of data that needs to be made available to all nodes. Using this type of network reduces the latency of waiting for the data to flow through the loop.

Another reason for using a distributed architecture is to maximize the processor bandwidth to perform the intensely-mathematical calculations necessary for computing strain. The strain calculation involves a 1,048,576 point discrete Fourier transform (DFT) and a series of smaller inverse DFTs. The software component which computes the strain from the raw data is one of the key parts of the system. Verification of its implementation is the subject of this report.

Measurement Apparatus

For purposes of verification, three sets of measurements were taken from a fiber containing 333 gratings. The fiber is bonded to a cantilevered aluminum bar (121.92 cm X 6.3 cm X 0.6 cm) mounted on a stand 10 cm above a bench top as illustrated in Figure 2. The fiber runs twice the length of the bar as indicated in Figure 3. The aluminum bar is also instrumented with 13 foil-type strain gauges that were not used for this test

Figure 2: *Aluminum bar mount on the bench top.*

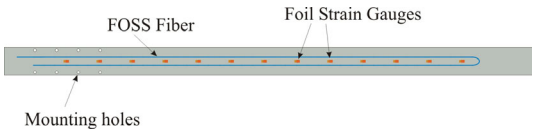

Figure 3: *Diagram of aluminum bar.*

One set of measurements was taken with no displacement applied to the cantilevered end resulting in the cantilevered end being about 10 cm from the bench top. A second data set was

taken with the cantilevered end depressed to approximately 1 cm from the bench top, and a third set was taken with the cantilever end raised to about 17 cm. Figure 4 shows the aluminum bar mounted on the test bench when the cantilever end is raised to about 17 cm.

Figure 4: *Cantilevered end raised.*

FOSS Strain Computation Algorithm

The FOSS computes strain at each grating location by extracting the wavelength of each grating's reflected signal. The algorithm computes the Fourier transform of the reflected signal to determine the location of each grating, then performs the inverse transform of each grating's signal to measure its modified wavelength. The FOSS strain-computing component (FSC) implements a modified version of the algorithm included in the FOSS technology detailed in [1]. The basic steps for computing the strain from the raw data are as follows:

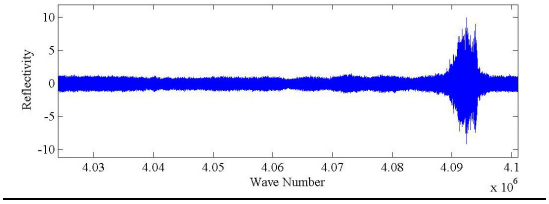

Figure 5: *Raw data.*

Step 1: *Convert raw data (Figure 5) from wave number domain to spatial domain by applying a DFT.*

$$F_k(d) = DFT(f_k(\mu)) \quad (1)$$

where:

- $f_k(\mu)$ is the raw data sampled by the data acquisition component. k is an index ranging from 1 to the sample size (1,048,576). $f_k(\mu)$ represents the response of the fiber in the wave number domain where wave number μ ranges from starting wave number (μ_s) to ending wave number (μ_e).
- $F_k(d)$ is the result of the DFT where k ranges from 1 to the sample size (1,048,576). $F_k(d)$ is the response of the fiber transformed into the spatial domain (d). See Figure 6.

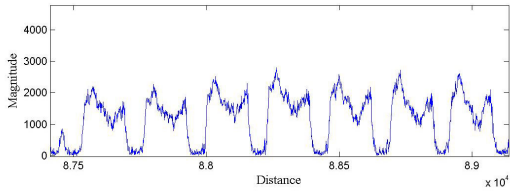

Figure 6: *An example of the magnitude of the DFT for the first few gratings of the data plotted in Figure 5.*

In the spatial domain, individual gratings can be identified in $F_k(d)$ by a set of grating location indexes (defined a priori). Step 2 through Step 9 are repeated for each grating.

Step 2: *Extract data for each grating.*

$$F_n(d) = F_k(d)\Big|_{k=gs}^{k=ge} \quad (2)$$

where:

- gs is the starting index for grating g.
- ge is the ending index for grating g

- $F_n(d)$ is the series of data points extracted for grating *g*. The symbol n ranges from 1 to the grating size defined by $(ge - gs)$.

Step 3: *Compute the reflectivity of the grating, in the wave number domain μ, by calculating the magnitude of the inverse DFT of the selected data segment relating to the specific grating. See Figure 7.*

$$f_n(\mu) = \left| IDFT(F_n(d)) \right| \quad (3)$$

where:

- $f_n(\mu)$ is the magnitude of the inverse FFT result for grating (*g*).

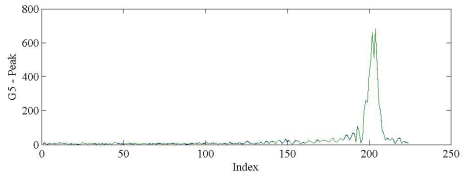

Figure 7*: Grating reflectivity.*

Step 4: *Filter the reflectivity data using a Butterworth low-pass filter. See Figure 8.*

$$B_n(\mu) = BW(f_n(\mu)) \quad (4)$$

where:

- $B_n(\mu)$ is the filtered peak for grating *g*.
- $BW()$ is an infinite impulse response (IIR) filter function using Butterworth coefficients applied to the grating peak $f_n(\mu)$ - equation (3). The filter function is a direct form II implementation of the standard difference equation with coefficient matrix A[] and B[] given by A=[1, -0.9824, 0.3477] and B[0.0913, 0.1826, 0.0913]

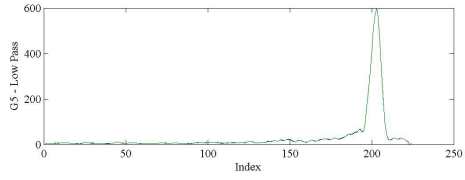

Figure 8: *Result of low-pass filter of grating reflectivity from Figure 7.*

The strain at each grating is computed from the wave number proportionally scaled to the index of the centroid of the grating peak shown in Figure 8. The centroid index was found to be very sensitive to the number of data points included in the centroid computation. For this reason, Step 5 has been added to the original algorithm to reduce the sensitivity of the centroid index to the number of data points included. A detailed study of this sensitivity is provided in a later section.

Step 5: *Between every two data points in $B_n(\mu)$, use linear interpolation to define one hundred $(E = 100)$ additional points to produce a bigger array.*

$$B'_m(\mu) = I(B_n(\mu)) \quad (5)$$

where:

- $B'_m(\mu)$ is the expansion of $B_n(\mu)$ hence m ranges from 1 to $(E \cdot n)$
- $I()$ is the interpolation function applied to $B_n(\mu)$.

Step 6: *Zero all data points in $B'_m(\mu)$ that are below the threshold defined by T ; where T is half of the highest value in $B_n(\mu)$ minus the average of $B_n(\mu)$ as given in equation (6).*

$$T = .5 \cdot \left(\max(B_n(\mu)) - \overline{B_n(\mu)}\right) \quad (6)$$

$$B''_m(\mu) = \begin{cases} 0 & : B'_m(\mu) < T \\ B'_m(\mu) & : B'_m(\mu) \geq T \end{cases} \quad (7)$$

Step 7: *Eliminate all peaks in the data except for the highest peak. This is accomplished by finding the index of the highest value; and searching forward and backward to the first point lower than the noise level of 0.0001; then setting all points beyond those points to zero. The result of this Step performed on Figure 8 is shown in Figure 9.*

$$t_m(\mu) = S(B''_m(\mu)) \quad (8)$$

where:

- $S()$ is the thresholding function as described in Appendix A.
- $t_m(\mu)$ is the portion of the grating peak (Figure 8) left after all the filtering and thresholding. This is the data left for calculating the centroid.

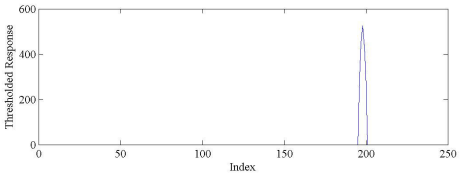

Figure 9: *Thresholded grating reflectivity.*

Step 8: *Compute the centroid* (ζ) *of* $t_m(\mu)$.

$$\zeta = \frac{\sum_{m=1}^{(E\cdot(g_e - g_s))}(m \cdot t_m(\mu))}{E \times \sum_{m=1}^{(E\cdot(g_e - g_s))} t_m(\mu)} \quad (9)$$

Step 9: *Use the centroid* (ζ) *to compute the centroid wave number* (μ_ζ)*given by:*

$$\mu_\zeta = \mu_s + \left(\frac{\zeta \cdot (\mu_e - \mu_s)}{(g_e - g_s)}\right) \quad (10)$$

where:

- μ_s is the wave number corresponding to the first data point.
- μ_e is the wave number corresponding to the last data point taken.

Step 10: *Convert the wave number to wavelength. Then use the wavelength to compute the strain relative to a baseline wavelength* (λ_b) .

$$\lambda = \frac{2\pi}{\mu_\zeta} \quad (11)$$

$$\mu Strain = \left(\frac{1e6}{0.79}\right) \cdot \left(\frac{\lambda - \lambda_b}{\lambda_b}\right) \quad (12)$$

A logging capability has been implemented in the FSC for recording various intermediate results in the algorithm. For this verification effort, the following were recorded:

- The DFT result from Step 1,
- The amplitude from the inverse DFT in Step 3,
- The filter result from Step 4,
- The grating centroid from Step 8,
- The micro-strain from Step 10.

Result Comparison

Verification of the FSC implementation is performed by comparing its results at various selected steps with the results from two other implementations: LabVIEW and MATLAB. For purposes of this verification, the LabVIEW implementation is considered the standard for comparison because it was adopted from the original FOSS development work. A MATLAB implementation was included to additionally

assess whether the MATLAB computing environment produces notable differences in results.

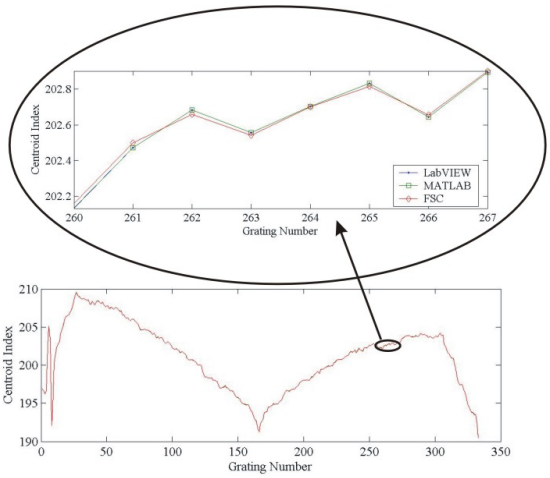

Figure 10: *Centroid computed by the three implementations.*

Computation of the grating-response centroid is shown in equation (9). The centroid is proportionally converted to a wave number between μ_s and μ_e. The centroid provides an index proportional to the wave number of the corresponding grating. Figure 10 shows the centroids computed by all three implementations for a single scan. The inset shows an expanded view of the centroids over a sub-region. The differences in centroid are shown in Figure 11. Several statistics for Figure 11 are given in Table 1.

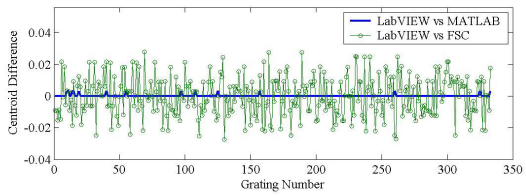

Figure 11: *Variation in centroid from the LabVIEW implementation versus MATLAB and versus FSC.*

As indicated in Table 1, the average difference in centroid for the FSC is 1.06×10^{-5} with a standard deviation of 1.25×10^{-2} while the average difference in centroid for the MATLAB implementation is 1.70×10^{-4} with a standard deviation of 6.20×10^{-4}.

To ensure that any observed difference is due solely to the centroid computation, identical grating peak data is supplied to each implementation, which in this case was the data produced by the FSC. An analysis of variance (ANOVA) was performed on the difference data shown in Figure 11. The results of the ANOVA show an 82% probability that the centroids computed by the different implementations are statistically the same.

Table 1: *Centroid differences between LabVIEW and MATLAB, and LabView and FSC.*

Centroid Compare	LabVIEW vs MATLAB	LabVIEW vs FSC
Max Difference	3.24×10^{-3}	2.81×10^{-2}
Min Difference	1.98×10^{-5}	-2.74×10^{-2}
Average Value	1.70×10^{-4}	1.06×10^{-5}
Standard Deviation	6.20×10^{-4}	1.25×10^{-2}

Finally, a comparison was made of the derived strain values as calculated in Step 10. Strain is derived by calculating the shift in reflected wavelength between a grating "at rest" (no tension or compression) and the wavelength returned from the same grating undergoing tension or compression. Sensitivity analysis reveals that the micro-strain computation in Step 10 is sensitive to the centroid determination, Step 8. This sensitivity is further discussed in the next section.

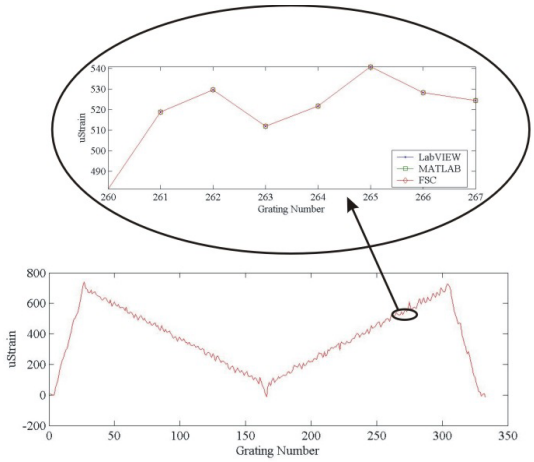

Figure 12: *Micro-Strain plot for all three implementations.*

The computed strain for all three models is shown in Figure 12. Like the centroid comparison, the micro-strain results from each of the three implementations differ. Again using the LabView implementation as reference, Figure 13 expands the micro-strain differences that are summarized in Table 2.

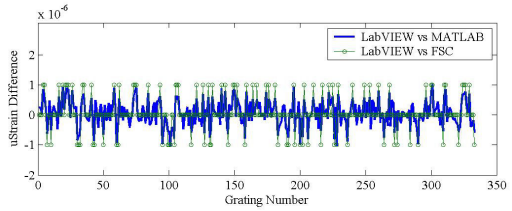

Figure 13: *Difference in micro-Strain computation.*

As indicated in *Table 2*, the average difference in µstrain for the FSC is 5.11×10^{-8} with a standard deviation of 5.38×10^{-7} while the average difference in µstrain for the MATLAB is 4.31×10^{-8} with a standard deviation of 4.35×10^{-7}.

To ensure that any observed difference is due solely to the micro-strain calculation algorithm, identical input centroid data is supplied to each implementation, which in this case was the data produced by the FSC. Again an ANOVA test was performed on the data in Figure 13. The test returned an 83% probability that the µstrain computed by the different implementations are statistically the same.

Table 2: *Micro-strain differences between LabVIEW and MATLAB, and LabView and FSC.*

uStrain Compare	LabVIEW vs MATLAB	LabVIEW vs FSC
Max Difference	1.02×10^{-6}	1.00×10^{-6}
Min Difference	-1.04×10^{-6}	-1.00×10^{-6}
Average Value	4.31×10^{-8}	5.11×10^{-8}
Standard Deviation	4.35×10^{-7}	5.38×10^{-7}

Strain Sensitivity

The FOSS strain computation is sensitive to the centroid index selection. Since there are often less than 10 data points available for computing the centroid after thresholding, the linear interpolation in Step 5 is used to add intermediate points to improve the centroid calculation. This was found to be particularly effective in cases where the signal contains points neighboring the threshold point. The resulting centroid could significantly change depending on whether or not such points are included or excluded from the calculation, resulting in a significant effect on the centroid index and ultimately the computed strain. Adding the interpolated points help to minimize the influence of border points.

To better understand the magnitude of strain error arising from an error in the centroid computation, the equation for computing µStrain can be put in terms of centroid index.

Examining Figure 14 and comparing to Equation (10) we can see that the term $(g_e - g_s)$ equals $(N-1)$, where (N) is the number of points in the array. Equation (10) becomes:

$$\mu_\zeta = \mu_S + (\zeta \cdot \delta) \tag{13}$$

where:

$$\delta = \frac{(\mu_e - \mu_s)}{(g_e - g_s)} \equiv \frac{(\mu_e - \mu_s)}{(N-1)} \tag{14}$$

Note that equation (14) represents the slope of the line that maps centroid to wave number. As illustrated in Figure 14, the range of possible values of (ζ) include all real numbers between 0 and $(N-1)$.

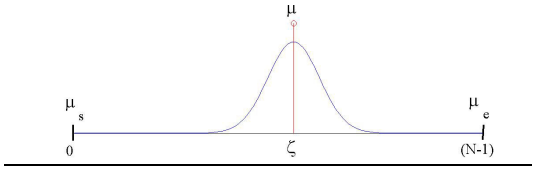

Figure 14: *Generic grating response.*

Substituting equations (14), (13), and (11) into (12), we get:

$$\mu Strain = \left(\frac{k \cdot \delta}{\mu_s + (\zeta \cdot \delta)} \right) \cdot (\zeta_b - \zeta) \tag{15}$$

where:

$$k = \left(\frac{1e6}{0.79} \right) \tag{16}$$

Table 3 shows typical values for several FOSS system parameters. Using these parameter values in equation (15) and comparing terms, we see that the term μ_s is more that 50 times greater than the term $(\zeta \cdot \delta)$. Using the previous result, we can say that $\mu_s >> (\zeta \cdot \delta)$.

Table 3: *FOSS system parameters.*

Parameters	Values
k	1265822.8
μ_s	652698.91
μ_e	640436.54
N	224
δ	54.988226

Equation [15] can then be approximated

$$\mu Strain \approx \left(\frac{k \cdot \delta}{\mu_s} \right) \cdot (\zeta_b - \zeta) \tag{17}$$

Assuming that the centroid (ζ) in [17] is the sum of the true centroid value and some error term $(\zeta_T \pm \zeta_E)$ would yield Equation [18].

$$\mu Strain \approx \left(\frac{k \cdot \delta \cdot (\zeta_b - \zeta_T)}{\mu_s} \right) \pm \left(\frac{k \cdot \delta \cdot \zeta_E}{\mu_s} \right) \tag{18}$$

Equation [19] isolates the error term for convenience.

$$\mu Strain_{Error} \approx \left(\frac{k \cdot \delta \cdot \zeta_E}{\mu_s} \right) \tag{19}$$

It is now possible to estimate the strain error introduced by errors in the centroid calculation using equation (19). Substituting the constant values from Table 3 into (19) we arrive at the result in (20). Note in (20) that the strain error is divided by the centroid to give the amount of micro-strain error per unit of centroid index.

$$\frac{\mu Strain_{Error}}{\zeta_E} \approx \left(\frac{k \cdot \delta}{\mu_s} \right) = 106.64236 \tag{20}$$

Based on this result, we conclude that every 0.01 unit error in centroid calculation approximately corresponds to 1 micro-strain error. Because of this 100:1 magnification, it is very important to estimate the centroid as precisely as possible. For this reason, **Step 5** was added to the algorithm to get a more precise estimate of the centroid.

Summary

This report briefly describes a system being developed at NASA Langley Research Center for

calculating in-situ strain measurements from a fiber with embedded Bragg gratings, and details steps taken to verify the correctness of an implementation of the demodulation calculations.

The verification was accomplished by comparing the intermediate computations of three implementations of the original LabView module reported in [1] – MATLAB, FSC, and LabView. The same algorithm was implemented in all three environments. For this effort, the original algorithm was augmented to include interpolation in the centroid selection procedure to reduce sensitivity to centroid calculation.

The centroid and strain results were calculated for each of the three implementations, and in general the centroid computations are in agreement. Statistics are provided relative to the FSC and MATLAB error estimates.

The work in this report is to verify that the FSC implements the FOSS algorithm with results comparable to the LabVIEW reference implementation. The validation of the FOSS algorithm is the subject of work in progress.

Acknowledgement

The authors would like to recognize and thank Jason Moore, one of the inventors of the original FOSS technology. Without his invention, this work would not exist and without his help, this report would not be as in-depth.

Appendix A: Pseudo-Code for Thresholding Function $S()$

The $S(f)$ function is a numerical technique for eliminating all but the highest peak in the signal f. It is better expressed in pseudo-code than a traditional math formulation. The steps to perform in the function are as given below.

```
Let fmax be the index of the max value of f

Start at the index of the highest value of f and
search backward for the first value that falls
below the noise threshold of 0.0001.   Set all
values of f beyond that point to zero.

found = false;
For (i=fmax; i>=0; i--) {
   If f(i)< .0001 {
         found = true;.
   }
   If (found == true) {
         f(i) = 0
   }
}

Start at the index of the highest value of f and
search forward for the first value that falls
below the noise threshold of 0.0001.   Set all
values of f beyond that point to zero.

found = false;
For (i=fmax; i<length(f); i++) {
   If f(i) < .0001 {
         found = true;.
   }
   If (found == true) {
         f(i) = 0
   }
}
```

References

[1] Mark Froggatt, Jason Moore, “Distributed Measurement of Static Strain in an Optical Fiber with Multiple Bragg Gratings at Nominally Equal Wavelengths”, Applied Optics-OT, Vol. 37 Issue 10 Page 1741 (April 1998)

REPORT DOCUMENTATION PAGE

Form Approved
OMB No. 0704-0188

1. REPORT DATE *(DD-MM-YYYY)*	2. REPORT TYPE	3. DATES COVERED *(From - To)*
01- 03 - 2005	Technical Memorandum	

4. TITLE AND SUBTITLE
Comparison of Fiber Optic Strain Demodulation Implementations

5a. CONTRACT NUMBER

5b. GRANT NUMBER

5c. PROGRAM ELEMENT NUMBER

6. AUTHOR(S)
Quach, Cuong C.; and Vazquez, Sixto L.

5d. PROJECT NUMBER

5e. TASK NUMBER

5f. WORK UNIT NUMBER
23-728-30-11

7. PERFORMING ORGANIZATION NAME(S) AND ADDRESS(ES)
NASA Langley Research Center
Hampton, VA 23681-2199

8. PERFORMING ORGANIZATION REPORT NUMBER
L-19071

9. SPONSORING/MONITORING AGENCY NAME(S) AND ADDRESS(ES)
National Aeronautics and Space Administration
Washington, DC 20546-0001

10. SPONSOR/MONITOR'S ACRONYM(S)
NASA

11. SPONSOR/MONITOR'S REPORT NUMBER(S)
NASA/TM-2005-213521

12. DISTRIBUTION/AVAILABILITY STATEMENT
Unclassified - Unlimited
Subject Category 35
Availability: NASA CASI (301) 621-0390

13. SUPPLEMENTARY NOTES
An electronic version can be found at http://ntrs.nasa.gov

14. ABSTRACT

NASA Langley Research Center is developing instrumentation based upon principles of Optical Frequency-Domain Reflectometry (OFDR) for the provision of large-scale, dense distribution of strain sensors using fiber optics embedded with Bragg gratings. Fiber Optic Bragg Grating technology enables the distribution of thousands of sensors immune to moisture and electromagnetic interference with negligible weight penalty. At Langley, this technology provides a key component for research and development relevant to comprehensive aerospace vehicle structural health monitoring. A prototype system is under development that includes hardware and software necessary for the acquisition of data from an optical network and conversion of the data into strain measurements. This report documents the steps taken to verify the software that implements the algorithm for calculating the fiber strain. Brief descriptions of the strain measurement system and the test article are given. The scope of this report is the verification of software implementations as compared to a reference model. The algorithm will be detailed along with comparison results.

15. SUBJECT TERMS
Fiber bragg gratings; OFDR; Structural health; Demodulation; Strain sensors

16. SECURITY CLASSIFICATION OF:			17. LIMITATION OF ABSTRACT	18. NUMBER OF PAGES	19a. NAME OF RESPONSIBLE PERSON
a. REPORT	b. ABSTRACT	c. THIS PAGE			STI Help Desk (email: help@sti.nasa.gov)
					19b. TELEPHONE NUMBER *(Include area code)*
U	U	U	UU	16	(301) 621-0390